

CONF-810831--102

FINAL

Conf-810831--102

DE83 007834

MODIFICATIONS OF SUBSURFACE ALLOY COMPOSITION
DURING HIGH-TEMPERATURE SPUTTERING*

N. Q. Lam and H. Wiedersich

Materials Science Division
Argonne National Laboratory
Argonne, Illinois, 60439, U.S.A.

The submitted manuscript has been authored by a contractor of the U. S. Government under contract No. W-31-109-ENG-38. Accordingly, the U. S. Government retains a nonexclusive, royalty-free license to publish or reproduce the published form of this contribution, or allow others to do so, for U. S. Government purposes.

July 1981

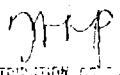
DISCLAIMER

This report was prepared as an account of work sponsored by an agency of the United States Government. Neither the United States Government nor any agency thereof, nor any of their employees, makes any warranty, express or implied, or assumes any legal liability or responsibility for the accuracy, completeness, or usefulness of any information, apparatus, product, or process disclosed, or represents that its use would not infringe privately owned rights. Reference herein to any specific commercial product, process, or service by trade name, trademark, manufacturer, or otherwise does not necessarily constitute or imply its endorsement, recommendation, or favoring by the United States Government or any agency thereof. The views and opinions of authors expressed herein do not necessarily state or reflect those of the United States Government or any agency thereof.

MASTER

To be presented at the Second Topical Meeting on Fusion Reactor Materials to be held August 9-12, 1981, Seattle, Washington.

*Work supported by the U.S. Department of Energy


DISTRIBUTION OF THIS DOCUMENT IS UNLIMITED

MODIFICATIONS OF SUBSURFACE ALLOY COMPOSITION DURING HIGH-TEMPERATURE SPUTTERING

N. Q. Lam and H. Wiedersich

Materials Science Division
Argonne National Laboratory
Argonne, Illinois, 60439, U.S.A.

Changes in the subsurface composition of concentrated binary alloys during high-temperature sputtering were studied using a kinetic model that includes Gibbsian adsorption, preferential sputtering, displacement mixing, radiation-enhanced diffusion, and radiation-induced segregation. Numerical solutions were obtained for Cu-Ni alloys under 5-keV Ar⁺ ion bombardment as functions of sputtering time and temperature. The effects of these various phenomena were examined in detail. The present calculations may be of importance in the areas of plasma contamination in fusion reactors, sputter depth-profiling, and elevated-temperature ion implantation.

1. INTRODUCTION

It has long been known that alloy surface compositions are altered by preferential sputtering and displacement mixing near room temperature to a depth approximately equal to the range of bombarding particles [1-3]. Despite this fact, sputtering with low-energy ions has been frequently used to obtain clean alloy surfaces, and combined with several different analytical techniques to profile the composition of multicomponent materials. At elevated temperatures, the subsurface composition of an ion-bombarded alloy can be modified by several additional phenomena. Aside from preferential sputtering and displacement mixing, Gibbsian adsorption, radiation-enhanced diffusion and radiation-induced segregation of alloying elements also take place. These phenomena not only affect the first-wall surface compositions and properties, but also influence the sputter rate and the composition of the sputtered material, and thus, play an important role in determining the plasma contaminate level in fusion systems. An understanding of sputter-induced compositional changes at high temperatures is therefore of technological importance. To date, only very limited information is available on this phenomenon, both experimentally [4,5] and theoretically [6,7].

In the present work, the effects of all the phenomena mentioned above on subsurface composition and sputtering rate of binary alloys have been investigated using a comprehensive model. The evolution of alloy composition in time and space as well as the sputtering rate were calculated as a function of irradiation temperature, time, and ion flux. Both the transient and steady states of the alloy composition were studied in detail.

2. FORMULATION OF THE PHENOMENOLOGICAL EQUATIONS

2.1 Basic Kinetics

The various phenomena considered in the present calculations are briefly described in this section. They are cast together into a kinetic model from which detailed information about their effects on subsurface alloy composition can be extracted using a suitable numerical technique.

2.1.1 Gibbsian Adsorption

Gibbsian adsorption is a segregation process caused by the reduction in surface or interface energy. Such segregation occurs thermally, and only involves a small perturbation to the distribution of alloying elements, extending to about one or two atomic layers. To describe this type of segregation, we consider the alloy as a medium of two phases: a "bulk phase" and a "surface phase". The latter is assumed to be confined to the surface plane of atoms. The equilibrium atom fractions of components A and B in the surface phase, C_A^s and C_B^s are related to the respective atom fractions in the bulk phase, C_A^b and C_B^b , by the equation [8]

$$\frac{C_A^s}{C_B^s} = \frac{C_A^b}{C_B^b} \exp(-\Delta H_a / kT) \quad (1)$$

where ΔH_a is the heat of adsorption, which represents the enthalpy change when an A-atom in the bulk phase exchanges positions with a B-atom in the surface phase.

During the concentration buildup towards equilibrium, the net flux of A-atoms into the surface atomic plane is defined as

$$\Omega j_A = (v_A^{bs} C_A^b C_B^s - v_A^{sb} C_A^s C_B^b) b \quad (2)$$

where b is the atomic layer thickness, Ω is the average atomic volume, and the surface-to-bulk jump frequency, v_A^{sb} , is related to the bulk-to-surface jump frequency, v_A^{bs} , by the following equation derived from the conditions of equilibrium

$$v_A^{sb} = v_A^{bs} \exp(-\Delta H_a/kT). \quad (3)$$

2.1.2 Preferential Sputtering

Concurrently with surface compositional changes resulting from Gibbsian adsorption, near-surface atoms are dislodged and ejected into the gas phase by energetic ion bombardment, leading to an erosion of the alloy surface. Since the sputtering coefficients of the alloying elements are likely to differ from each other, atoms of different elements are sputtered off with different probabilities, which gives rise to the preferential sputtering phenomenon.

As a result of atomic collisions, surface atoms of the two components are sputtered off at rates per unit area

$$\frac{dN_A}{dt} = \phi S_A C_A^S \quad (4)$$

and

$$\frac{dN_B}{dt} = \phi S_B C_B^S = \phi S_B (1 - C_A^S) \quad (5)$$

Here, ϕ is the ion flux (ions/cm²s), and S_A and S_B are the sputtering coefficients of A- and B-components, respectively, i.e., the numbers of target atoms sputtered per incident ion per unit concentration.

The total rate at which atoms of both constituents are removed per unit area is thus

$$\frac{dN}{dt} = \phi [S_A C_A^S + S_B (1 - C_A^S)] \quad (6)$$

Consequently, the surface recedes at a sputtering rate

$$\dot{\delta} = \frac{d\delta}{dt} = \Omega \frac{dN}{dt} = \phi \Omega [S_A C_A^S + S_B (1 - C_A^S)] \quad (7)$$

where δ is the thickness of the surface layer removed by sputtering.

2.1.3 Displacement Mixing

Similar to sputtering, the inter-mixing of alloying elements is induced by displacement cascades generated by the passage of the primary ion. These cascades contribute to sputtering if they take place near the alloy surface. A simplified description of ion bombardment-induced mixing can be formulated within a diffusion model.

We first define the effective displacement-induced diffusion coefficient

$$D_A^* = D_B^* = Zb^2 K_0 \eta / 6 \quad (8)$$

where Z is the coordination number, K_0 is the spatially-dependent damage rate (number of displacements per atom per second, dpa/s) and η is the number of atoms changing sites per dpa. The net flux of A-atoms across a fixed "lattice" plane can be approximated by

$$\Omega J_A^* = -D_A^* \nabla C_A. \quad (9)$$

The product $K_0 \eta$ and, hence, the effective diffusion coefficient D_A^* in eq. (8) are assumed to be temperature independent, i.e., displacement mixing is assumed to be an athermal process.

2.1.4 Radiation-enhanced Diffusion

In addition to sputtering off near-surface atoms, the bombarding particles also produce damage within the solid, creating point defects and displacement cascades in a random fashion. Below $\sim 0.6 T_m$ (T_m is the absolute melting temperature), the concentrations of radiation-induced vacancies (v) and interstitials (i) can exceed their thermodynamic equilibrium values by several orders of magnitude. Since the average diffusion coefficients of A- and B-atoms in the alloy are proportional to the concentrations of point defects, i.e., [9]

$$D_A = d_{Av} C_v + d_{Ai} C_i \quad (10)$$

and

$$D_B = d_{Bv} C_v + d_{Bi} C_i,$$

diffusion of the alloying elements is strongly enhanced by irradiation at temperatures where point defects are mobile. The diffusivity coefficients d_{Av} , d_{Bv} , d_{Ai} , and d_{Bi} in eqs. (10) contain the kinetic characteristics for diffusion of the elements A and B via vacancies and interstitials, respectively [9].

2.1.5 Radiation-induced Segregation

At sufficiently high temperatures, mobile point defects that escape mutual recombination anneal out by diffusion to sinks. Since defect fluxes to sinks are associated with fluxes of atoms, any preferential association of defects with a particular alloying element and/or preferential participation of a component in defect diffusion will couple a net flux of the alloying element to the defect fluxes. This preferential flux coupling leads to a compositional redistribution in irradiated alloys, a phenomenon called radiation-induced segregation.

In a concentrated binary alloy AB, the fluxes of atoms and defects with respect to a coordinate system fixed on the crystal lattice are defined as [9]

$$\begin{aligned}\Omega J_A &= -D_A \alpha \nabla C_A - C_A (d_{Ai} \nabla C_i - d_{Av} \nabla C_v) \\ \Omega J_B &= -D_B \alpha \nabla C_B - C_B (d_{Bi} \nabla C_i - d_{Bv} \nabla C_v) \\ \Omega J_v &= (d_{Av} - d_{Bv}) \alpha C_v \nabla C_A - D_v \nabla C_v\end{aligned}\quad (11)$$

and

$$\Omega J_i = (d_{Ai} - d_{Bi}) \alpha C_i \nabla C_A - D_i \nabla C_i$$

where α is the thermodynamic factor which takes care of the difference between the concentration gradient and the chemical potential gradient. The atom fluxes are induced by the chemical-composition gradient, as well as by the vacancy and interstitial concentration gradients. Similarly, the defect fluxes are driven by the A- and B-atom concentration gradients and by their own gradients. It has been established [9] that depletion of the A component occurs at a sink when $d_{Av}/d_{Bv} > d_{Ai}/d_{Bi}$, i.e., when the preferential transport of A-atoms via vacancies outweighs that via interstitials. Conversely, enrichment of A-atoms at the sink takes place when $d_{Av}/d_{Bv} < d_{Ai}/d_{Bi}$.

2.2 General Kinetic Equations

Taking into account the effects of all the phenomena described in section 2.1, one can express the evolution of atom and defect distributions in time and space by the following set of coupled partial differential equations:

$$\frac{\partial C_v}{\partial t} = -\nabla J_v + K_0 - R \quad (12a)$$

$$\frac{\partial C_i}{\partial t} = -\nabla J_i + K_0 - R \quad (12b)$$

and

$$\frac{\partial C_A}{\partial t} = -\nabla (J_A^* + J_A) \quad (12c)$$

where K_0 and R are the total local rates of production and recombination of vacancies and interstitials. The equation for B-atoms is unnecessary because it is not independent, i.e., $C_B = 1 - C_A$.

The time-dependent atom and defect concentration profiles can be determined by solving eqs. (12) numerically for appropriate initial and boundary conditions [10]. Equation (2) describing Gibbsian adsorption must be included into Eq. (12c) when the concentrations of A-atoms in the first two atomic layers are calculated. Also, eq. (7), which describes the C_A^S -dependence of the sputtering rate is coupled to this system of equations through an appropriate mathematical transformation of the physical space [6,7]. Hence, the numerical solution also yields the time dependence of the sputtering rate as well as the total erosion of the sputtered surface.

3. SAMPLE CALCULATIONS

The calculations were performed for concentrated Cu-40 at.% Ni alloys, for which reliable experimental measurements have been reported [4-5]. Cu-atoms were assumed to migrate by preferential exchange with vacancies. The energies of vacancy migration via Cu- and Ni-atoms were taken to be those representative of the pure metals, 0.77 [11], and 1.08 eV [12], respectively. The interstitial migration energy was taken to be 0.12 eV [13], the same for both alloying elements. To include Gibbsian adsorption, a heat of adsorption of -0.25 eV [8] was used for Cu-atoms. Sputtering and damage production by 5-keV Ar⁺ ions were considered. The sputtering coefficients for Cu and Ni were 5.5 [14] and 2.75 atoms/ion, respectively; the latter value was obtained using the experimentally-determined ratio $S_{Cu}/S_{Ni} = 2$ [5]. The same damage distribution for 5-keV Ar⁺ ions was used in the present work as described in previous papers [6,7]. The peak damage occurs at 0.7 nm and the total range is ~ 3 nm. An ion flux of 2.5×10^{14} ions/cm²s (i.e., 40 μ A/cm²) was considered, yielding a peak-damage rate of 1 dpa/s.

To understand the time evolution of the surface concentration at different temperatures, we first discuss the effects of the various phenomena. Figure 1 shows the time dependence of the Cu concentration at the alloy surface, calculated for different combinations of processes at 400°C. Without irradiation, Gibbsian adsorption leads to a strong Cu enrichment (up to 99.1 at.%) in the first surface atom layer (curve 1). With irradiation, if only preferential sputtering and radiation-enhanced diffusion are taken into account (curve 2), the surface concentration of Cu, C_{Cu}^S , decreases monotonically to the steady-

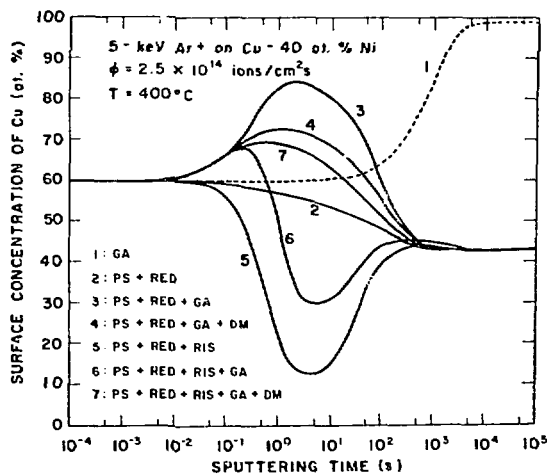


Fig. 1. Effects of various combinations of the five basic processes on the time evolution of the surface concentration of Cu during sputtering at 400°C.

state value defined by the sputtering coefficient ratio and the bulk composition

$$\left(\frac{C_{Cu}^S}{C_{Ni}^S} \right)_{ss} = \frac{S_{Ni}}{S_{Cu}} \cdot \frac{C_{Cu}^b}{C_{Ni}^b} \quad (13)$$

A true steady state is attained only when the rate of loss of Cu- and Ni-atoms from the surface altered layer is balanced by a corresponding gain from the bulk as the altered layer recedes into the alloy. At steady state, $C_{Cu}^S = 42.86$ at.%. Now, if Gibbsian adsorption is also included (curve 3), C_{Cu}^S increases rapidly at short bombardment times (< 1 s) due to radiation-enhanced adsorption, and then decreases slowly to the steady-state value. The inclusion of displacement mixing reduces the effect of Gibbsian adsorption (curve 4). On the other hand, if one considers only preferential sputtering, radiation-enhanced diffusion, and radiation-induced segregation (curve 5), C_{Cu}^S decreases at short sputtering times due to the dominant effect of segregation. However, as the bombardment time increases, the quasi-steady-state C_{Cu}^S , set up by segregation, is gradually altered by preferential sputtering, and C_{Cu}^S increases to the steady-state value. If Gibbsian adsorption is also allowed to occur in addition (curve 6), then one can distinguish three stages in the modification of surface composition: dominant radiation-enhanced Gibbsian adsorption, causing an increase in C_{Cu}^S at short times, followed by dominant radiation-induced segregation, and then preferential sputtering. And finally, with the addition of displacement mixing (curve 7), i.e., if all the processes are included, the effect of radiation-induced segregation is masked; C_{Cu}^S increases initially and then decreases towards the steady-state value. Compared to curve 4, curve 7 is lowered by radiation-induced segregation during the transient state.

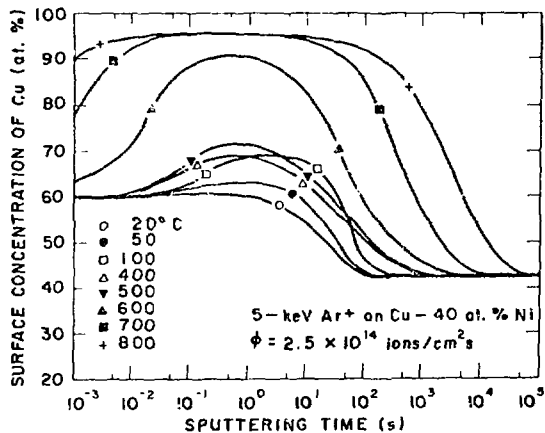


Fig. 2. Time dependence of Cu concentration at the alloy surface during sputtering at different temperatures.

The time evolution of C_{Cu}^S is plotted in Fig. 2 for various temperatures. Near room temperatures, enhanced Gibbsian adsorption is negligible, C_{Cu}^S changes slowly to the steady-state value. With increasing temperatures, the effect of Gibbsian adsorption becomes stronger, C_{Cu}^S increases more rapidly at short sputtering times, and decreases to the steady-state value at longer times. The time required to attain steady state increases from 10^2 to 5×10^4 s when the temperature increases from 20 to 800°C . This is in good agreement with recent experimental measurements [4].

The dependence of the sputtering rate on sputtering time and temperature is illustrated in Fig. 3. Since the sputtering rate is proportional to C_{Cu}^S (eq. 7), this dependence is similar to that of C_{Cu}^S , shown in Fig. 2. The initial and steady-state sputtering rates are 1.26 and 1.11 $\text{\AA}/\text{s}$, respectively.

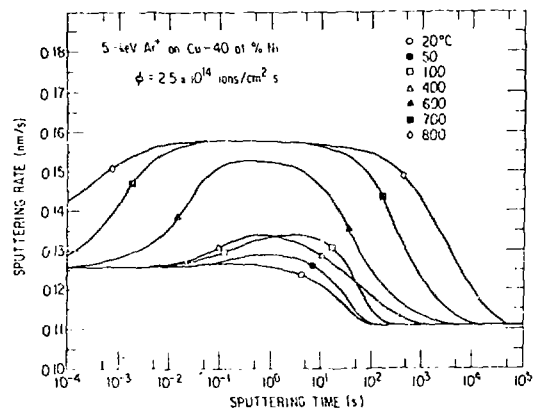


Fig. 3. Time dependence of sputtering rate calculated for various temperatures.

Figure 4 shows the steady-state concentration profiles in the near-surface region calculated for various temperatures. The logarithmic scale has been used for the distance from the sputtered surface to effectively show the compositional variations in the first two atomic layers, each 2.06 \AA thick. For all the temperatures studied, the steady state Cu concentration in the first atomic plane is controlled by preferential sputtering (eq. 13). Below 100°C , where point-defect mobility is limited, preferential sputtering and displacement mixing govern the development of the alloy composition in the altered layer, which extends to a depth approximately equal to that of the damage range. The alloy composition within this altered layer is rather uniform. Above 100°C , Gibbsian adsorption, radiation-enhanced diffusion, and radiation-induced segregation become significant, and effectively determine the extent of and the composition in

REFERENCES

- [1] Gillam, E., The penetration of positive ions of low energy into alloys and composition changes produced in them by sputtering, *J. Phys. Chem. Solids* 11 (1959) 55-67.
- [2] Ho, P. S., Lewis, J. E., Wildman, H. S., and Howard, J. K., Auger study of preferred sputtering on binary alloy surfaces, *Surface Sci.* 57 (1976) 393-405.
- [3] Koshikawa, T., Goto, K., Saeki, N., Shimizu, R., and Sugata, E., Preferential sputtering of Cu-Ni alloys at low temperature using lower energy Auger electron spectra, *Surface Sci.* 79 (1979) 461-469.
- [4] Rehn, L. E., Danyluk, S., and Wiedersich, H., Sputter-induced subsurface segregation in a Cu-Ni alloy, *Phys. Rev. Lett.* 43 (1979) 1764-1767.
- [5] Rehn, L. E., and Wiedersich, H., Sputter-induced modification of alloy composition in near-surface regions, *Thin Solid Films* 73(1980)139-143
- [6] Lam, N. Q., Leaf, G. K., and Wiedersich, H., Effects of radiation-induced segregation and preferential sputtering on the sputtering rate of alloys, *J. Nucl. Mater.* 85 & 86 (1979) 1085-1089.
- [7] Lam, N. Q., Leaf, G. K., and Wiedersich, H., Sputter-induced surface composition changes in alloys, *J. Nucl. Mater.* 88 (1980) 289-298.
- [8] Wynblatt, P. and Ku, R. C., Surface segregation in alloys, in Johnson, W. C. and Blakely, J. M. (eds), *Interfacial Segregation* (American Society for Metals, Metals Park, Ohio, 1979).
- [9] Wiedersich, H., Okamoto, P. R., and Lam, N. Q., A theory of radiation-induced segregation in concentrated alloys, *J. Nucl. Mater.* 83 (1979) 98-108.
- [10] Lam, N. Q., and Wiedersich, H., to be published.
- [11] Berger, A. S., Ockers, S. T., and Siegel, R. W., Measurement of the monovacancy formation enthalpy in copper, *J. Phys.F: Metal Physics* 9 (1979) 1023-1033.
- [12] Smedskjaer, L. C., Fluss, M. J., Legnini, D. G., Chason, M. K., and Siegel, R. W., The vacancy formation enthalpy in Ni determined by positron annihilation, 1981, to be published in *J. Phys. F: Metal Physics*.
- [13] Young, F. W., Interstitial mobility and interactions, *J. Nucl. Mater.* 69 & 70 (1978) 310-330.
- [14] Maissel, L. I., Application of sputtering to the deposition of films, in Maissel, L.I. and Glang, R. (eds.), *Handbook of Thin Film Technology* 4-1 (McGraw-Hill, New York, 1970).

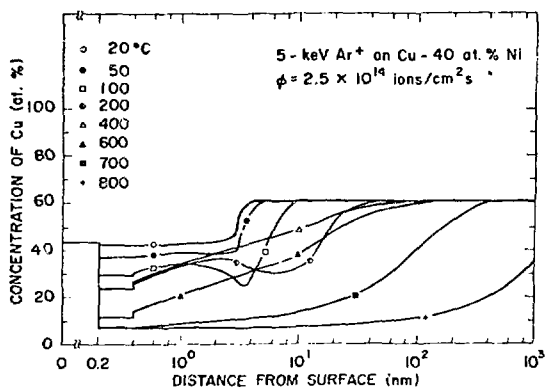


Fig. 4. Steady-state Cu concentration profiles in a Cu-40 at.% Ni alloy sputtered at different temperatures.

the altered layer; the higher the temperature, the thicker the altered layer. At 800°C, for example, the thickness of this layer is $\sim 3 \mu\text{m}$, which is ~ 1000 times larger than the damage range. This is consistent with the experimental measurements by Rehn et al. [4,5] using Auger electron spectroscopy. Compositional changes at such large depths suggest that an appreciable enhancement of diffusion occurs because of sputter-induced point defects. It is the extension of the concentration gradient to such depths that results in the long times which are necessary to reach steady state at high temperatures.

4. CONCLUDING REMARKS

The present calculations were performed for sputter-etching conditions, i.e. a high flux of heavy ions, because reliable experimental data are available. However, the model can be applied to any low-energy ion bombardment situation, e.g., sputtering with D^+ , T^+ , and He^{++} ions in fusion reactors, provided that the damage distribution and partial sputtering coefficients are known. The general trends in the subsurface-composition changes reported here will remain the same; the magnitudes will, of course, be different owing to different dose rates and sputtering coefficients. The buildup time to steady state increases with decreasing ion flux [7,10]. However, the total amount of material removed before steady state is reached is approximately flux independent.

ACKNOWLEDGEMENTS

The authors acknowledge informative discussions with Dr. L. E. Rehn, and comments of Dr. R. W. Siegel on the manuscript. This work is supported by the U.S. Department of Energy.